Cellular and Molecular Life Sciences (2024) 81:424
https://doi.org/10.1007/s00018-024-05454-2



ORIGINAL ARTICLE

# NPRL2 promotes TRIM16-mediated ubiquitination degradation of Galectin-3 to prevent CD8$^+$T lymphocyte cuproptosis in glioma

Feng Wang[1] · Jianhe Yue[1] · Maoxin Zhang[1] · Maoyuan Sun[1] · Xu Luo[1] · Hao Zhang[1] · Yuanyuan Wu[2] · Yuan Cheng[1] · Jin Chen[1] · Ning Huang[1]

Received: 17 June 2024 / Revised: 9 September 2024 / Accepted: 19 September 2024


## Abstract

**Background** Our previous study found that tumor suppressor nitrogen permease regulator like-2(NPRL2) is frequently downregulated in glioma, leading to malignant growth. However, NPRL2-mediated crosstalk between tumor cells and immune cells remains unclear.

**Methods** The regulatory effects of NPRL2 on tripartite motif–containing protein 16(TRIM16) dependent ubiquitination degradation of Galectin-3(Gal-3) were explored. The effects of Gal-3 on copper uptake, immunocompetence and cuproptosis were investigated in CD8$^+$T lymphocytes(CD8$^+$T cells). The ability of NPRL2 to protect CD8$^+$T cells from Gal-3 damage was evaluated. Furthermore, the correlations among NPRL2, TRIM16, Gal-3 and CD8$^+$T cell accumulation were analyzed in glioma clinical specimens.

**Results** NPRL2 increased the TRIM16 expression via inactivation of ERK1/2, which in turn promoted the ubiquitination-mediated degradation of Gal-3 and diminished Gal-3 release from glioma cells. Moreover, Gal-3 accelerated copper uptake and triggered cuproptosis in CD8$^+$T cells, whereas NPRL2 increased CD8$^+$T cell recruitment and prevented impairment of CD8$^+$T cells by Gal-3. Clinical samples revealed that NPRL2 expression was positively associated with TRIM16 expression and negatively correlated with Gal-3, but Gal-3 expression was negatively associated with CD8$^+$T cell accumulation.

**Conclusion** Glioma-derived NPRL2/TRIM16/Gal-3 axis participates in the regulation of CD8$^+$T cell cuproptosis, which provides a promising strategy to rescue the immune activity of CD8$^+$T cells and reverse immunosuppression in glioma.

**Keywords** Glioma · CD8$^+$T lymphocyte · Nitrogen permease regulator like-2 · Tripartite motif–containing protein 16 · Galectin-3 · Cuproptosis

## Abbreviations

| | |
|---|---|
| CCK-8 | Cell counting kit-8 |
| CD8$^+$T cell | CD8$^+$T lymphocyte |
| CHX | Cycloheximide |
| CM | Conditioned medium |
| CO-IP | Co-Immunoprecipitation |
| CTR1 | Copper transporter 1 |
| Cu | Copper |
| DLAT | Dihydrolipoamide S-Acetyltransferase |
| DMEM/F12 | Dulbecco's modified Eagle's medium/ Ham's nutrient mixture F-12 |
| ELISA | Enzyme-linked immunosorbent assay |
| ERK | Extracellular regulated protein kinase |
| FBS | Fetal bovine serum |
| FCM | Flow cytometry |
| FDX1 | Ferredoxin 1 |
| Gal-3 | Galectin-3 |
| GAPDH | Glyceraldehyde-3-phosphate dehydrogenase |
| HSP70 | Heat shock protein 70 |
| IF | Immunofluorescence |
| IFN-γ | Interferon gamma |

✉ Jin Chen
chenjin@hospital.cqmu.edu.cn

✉ Ning Huang
304237@hospital.cqmu.edu.cn

[1] Department of Neurosurgery, The Second Affiliated Hospital of Chongqing, Medical University, 74 Linjiang Rd, Yuzhong, Chongqing 400010, China

[2] Department of Health Medicine Center, The Second Affiliated Hospital of Chongqing Medical University, Chongqing, China

Published online: 05 October 2024

| | |
|---|---|
| IHC | Immunohistochemistry |
| IL-2 | Interleukin-2 |
| MACS | Magnetic activated cell sorting |
| NC | Negative control |
| NPRL2 | Nitrogen permease regulator like-2 |
| OD | Optical density |
| PVDF | Polyvinylidene fluoride |
| TCA | Tricarboxylic acid cycle |
| TME | Tumor microenvironment |
| TRIM16 | Tripartite motif–containing protein 16 |
| TSG | Tumor suppressor gene |
| TUSC4 | Tumor suppressor candidate 4 |
| UB | Ubiquitin |
| WB | Western blot |

## Introduction

Immunotherapy, a revolutionary strategy, has transformed the landscape of cancer treatment and achieved great improvement in outcomes for many tumors, but glioma is a conspicuous exception to this trend owing to the properties of immune-cold tumor [1]. Due to genetic mutations associated with tumor progression, glioma cells produce and secrete abnormal levels of cytokines, chemokines and extracellular proteins into the tumor microenvironment(TME), leading to the scarcity and dysfunction of infiltrating antitumor lymphocytes [2, 3]. Thus, glioma has emerged as a model for immunosuppression and immune evasion [4].

Our previous studies have identified that nitrogen permease regulator like-2(NPRL2), also known as tumor suppressor candidate 4(TUSC4), is a potential tumor suppressor gene(TSG) and conducive to antiproliferative effects, but downregulation of NPRL2 occurs frequently in glioma, resulting in malignant growth [5]. Recently, some articles reported that NPRL2 regulated the ubiquitin(UB)-proteasome system and hindered tumorigenicity [6]. Ubiquitination is orchestrated by cascade of E1 UB-activating enzymes, E2 UB-conjugating enzymes and E3 UB ligases, and serves as a crucial posttranslational modification of protein substrates [7]. E3 ligases play the most pivotal role in whole ubiquitination process because of their ability to accurately select, bind and label target proteins for degradation [8]. However, E3 ligases are dysfunctional in many cancers so that the expression and activation of their target proteins are abnormal, and antitumor immunity is disturbed [9, 10].

Tripartite motif–containing protein 16(TRIM16) belongs to the TRIM family. Unlike other members, TRIM16 lacks the classic RING finger domain but has a B-box domain, which exerts E3 ligase activity [11]. Increasing evidence has documented that TRIM16 inhibits tumor progression via ubiquitination function [12, 13]. Galectin-3(Gal-3) is positioned in extracellular space, cytoplasm and nucleus. Specifically, tumor cells release Gal-3 to impede recruitment and impair the cytotoxic activity of $CD8^+$T lymphocytes($CD8^+$T cells), thereby maintaining an immunosuppressive TME [14, 15]. In contrast, depletion of Gal-3 potentiates immunotherapy responses and tumor rejection, including in glioma [16, 17]. Some studies have confirmed that TRIM16 was able to bind Gal-3, and Gal-3 could be degraded by the UB–proteasome system to sensitize tumor immunotherapy [18, 19]. However, it has not been elucidated whether TRIM16 triggers ubiquitination degradation of Gal-3 for immunomodulation in glioma.

Copper(Cu) is an essential trace element and maintains a dynamic balance at extraordinarily low intracellular levels via copper importer copper transporter 1 (CTR-1) and copper exporters ATPase copper transporting alpha (ATP7A) and beta (ATP7B) [20]. However, excess copper damages tricarboxylic acid cycle (TCA) in mitochondrial respiration and stimulates cuproptosis with distinctive loss of lipoylated and iron-sulfur(Fe-S) cluster proteins as well as an increase in heat shock protein 70(HSP70) levels [21]. In fact, cuproptosis is correlated with an immunosuppressive TME [22].

In this study, the effects of NPRL2 on the TRIM16-mediated ubiquitination degradation of Gal-3 were evaluated in glioma cells. Furthermore, this is the first report to explore whether extracellular Gal-3 stimulates $CD8^+$T cell cuproptosis. Our findings supported that the regulation of NPRL2/TRIM16/ Gal-3 axis leads to novel strategies for restoring antitumor immunity in glioma by preventing $CD8^+$T cells from cuproptosis.

## Materials and methods

### Reagents and primary antibodies

Primary antibodies against NPRL2, Gal-3 and GAPDH were obtained from Santa Cruz Biotechnology (CA, USA). TRIM16, CTR1, HSP70, ferredoxin 1(FDX1), dihydrolipoamide S-acetyltransferase(DLAT) were purchased from Thermo Fisher Scientific(HK, China). Total-ERK1/2, phospho-ERK1/2(p-ERK1/2), CD8, HA-tag, Flag-tag and His-tag were bought from Abcam(MA, USA). MG132 and IgG were purchased from Beyotime Biotechnology(Shanghai, China). Elesclomol, cycloheximide(CHX) and ERK1/2 activator BAY2965501(α-ERK) were purchased from MedChem Express(NJ, USA). The recombinant mouse His-tag Gal-3 protein was obtained from Abcam, $CuCl_2$ was purchased from Sigma(Shanghai, China).

## Cell culture

Dulbecco's modified Eagle's medium/Ham's nutrient mixture F-12 (DMEM/F12), RPMI-1640 and fetal bovine serum (FBS) were purchased from Gibco(CA, USA). Two mouse glioma cell lines(GL261 and CT-2 A) were obtained from the Shanghai Life Academy of Sciences Cell Library(Shanghai, China) and cultured in DMEM/F12 plus 10% FBS. CD8$^+$T cell isolation from mice was approved by the Ethics Committee of Chongqing Medical University. As described previously, the spleens of mice were collected after anesthesia via injection of 2% pentobarbital into the abdomen. After being minced and digested, the spleen fragments were added to Ficoll–Paque (Sigma, MO, USA) and centrifuged(500 ×g, 30 min, 20℃), the mononuclear cell layer was extracted. The CD8$^+$T cells were purified via magnetic activated cell sorting (MACS) according to manufacturer's protocol(Miltenyi Biotec, Germany), cultured in RPMI-1640 supplemented with 10% FBS, and activated by 2 μg/ml anti-CD3/anti-CD28 antibodies(BD Biosciences, NJ, USA) for 48 h [23]. All the cells were maintained in 5% $CO_2$ at 37℃.

## Cell transfection

The NPRL2 overexpression lentiviral vector(LV-NPRL2) and corresponding negative control lentivirus (NC), as well as the lentiviral TRIM16 shRNA vector(TRIM16-shRNA-LV) and matched empty lentivirus (NC1) were purchased from Genechem(Shanghai, China).The HA-tag UB plasmid was purchased from Miaoling Biology(Wuhan, China), and the Flag-tag TRIM16 plasmid was purchased from Dowobio Biotechnology(Shanghai, China). Cell transfection and transduction were performed as previously described according to the manufacturer's protocol [5]. The medium from two glioma cell lines in control, NC and LV-NPRL2 groups cultured for 48 h was collected as conditioned medium(CM), such as CM-control, CM-NC and CM- LV, respectively.

## Real-time PCR

Total RNA was extracted from two glioma cell lines using RNAiso Plus (Invitrogen, CA, USA). The concentrations of RNA samples were measured via a spectrophotometer, and the RNA was reverse-transcribed into cDNA via the Primescript RT reagent Kit (TaKaRa Biotechnology, Beijing, China). The primer sequence for Gal-3 was as follows: forward 5'-AACACGAAGCAGGACAATAA CTGG-3' and reverse 5'-GCAGTAGGTGAGCATCGTTGAC-3'. For GAPDH was: 5'-CATCACTGCCACCCAGAAGAC TG-3' and reverse 5'-ATGCCAGTGAGCTTCCCGTTCA G-3'. The amplification conditions were as follows: 95℃ for 20 s, followed by 40 cycles at 95℃ for 15s, and 60℃ for 60s. Relative fold-changes in mRNA levels were determined via the $2^{-\Delta\Delta CT}$ method [5].

## Western blot(WB)

WB analysis was performed as previously described [24]. Briefly, the cells were collected and lysed in RIPA lysis buffer containing 0.1% phosphatase inhibitor and 1%PMSF. The 30 μg protein samples were separated by SDS–PAGE and transferred onto PVDF membranes. The primary antibodies were used to incubate with PVDF membranes overnight at 4℃, including NPRL2(1:200), Gal-3(1:500), GAPDH(1:1000), TRIM16(1:200), HA(1:100), Flag(1:100), His(1:100), p-ERK1/2(1:200), total-ERK1/2(1:500), CTR1(1:200), HSP70(1:200), DLAT(1:300) and FDX1(1:400). PVDF membranes were incubated with the secondary antibodies(1:5000) for 1 h at 37℃, and the protein in each band was quantified using Quantity One 4.6 computer software.

## Enzyme-linked immunosorbent assay (ELISA)

The medium was collected after culturing with glioma cells for 48 h. Then, Gal-3, interleukin-2(IL-2) and interferon gamma(IFN-γ) levels were calculated according to optical density values by an enzyme-labelled instrument. ELISA was performed following manufacturer's instructions.

## Coimmunoprecipitation (Co-IP)

The cells were lysed on ice using NP40 buffer containing a protease inhibitor. Total protein(60 μg) was divided equally. 30 μg of protein was used as input, and the other 30 μg was put into protein G-agarose beads(Thermo Fisher Scientific, MA, USA) which were pretreated with 2 μl of capturing antibodies, such as IgG, Gal-3, Flag or CTR1. After overnight incubation at 4℃, the beads were washed, and the final samples were used for WB analysis.

## Ubiquitination assays

The ubiquitination of Gal-3 was required for transfection with HA-tag UB plasmid, and the cells were treated with 10μM MG132 for 6 h before collection. Then, the cells were lysed and subjected to Co-IP via anti-IgG or anti-Gal-3 agarose beads and subsequent SDS-PAGE. Ubiquitination of Gal-3 was detected using HA antibody(1:100).

## Immunofluorescence(IF)

Glioma cells were seeded onto coverslips for attachment overnight. The $CD8^+$T cell suspension was dropped onto slides coated with poly-lysine, and additional medium was added after 4 h for culturing these cells overnight. Then, the cells were fixed, blocked, and incubated with primary antibodies(against Gal-3 at 1:200, TRIM16 at 1:200, His at 1:100 and CTR1 at 1:100) overnight at 4℃. Next, the cells were incubated with FITC and TRITC-labelled secondary antibodies together with DAPI for IF.

## Cell counting kit-8(CCK-8)

$CD8^+$T cells were seeded into 96-well plates at a density of 4000 cells/well. After incubation with recombinant mouse Gal-3 protein, $CuCl_2$, elesclomol or treatment with different CM for 24, 48–72 h, CCK-8 buffer(10 µl) was added to each well for 20 min. Absorbance values were calculated using an enzyme labelled instrument (450 nm).

## Flow cytometry(FCM)

After incubation with the Gal-3 protein for 48 h, the $CD8^+$T cells were harvested, resuspended and stained with Annexin V-FITC/PI apoptosis reagent kit(KeyGen Biotechnology, Nanjing, China). Early apoptosis was observed by flow cytometry.

## Copper microplate assay

The copper assay kit(Abcam) was used to detect copper content according to user' manual. The $CD8^+$T cells($2\times10^6$) were harvested and lysed to analyze copper concentration via an enzyme labelled instrument (360 nm).

## Intracranial tumor model

Following previous studies, C57BL/6 male mice (5–6 weeks) were used to establish brain tumor model [23]. After anesthetization and sterilization on a stereotaxic instrument, the mouse glioma cells were injected at 1.25 mm right lateral and cranium 0.7 mm anterior to the bregma as well as at a depth of 2.5 mm from the brain surface. The tumors were created and collected after 21d.

**Table 1** Clinical characteristics of 93 patients

| | *n* | % |
|---|---|---|
| Gender | | |
| Male | 48 | 51.61 |
| Female | 45 | 48.39 |
| Age(years) | | |
| >45 | 52 | 55.91 |
| ≤45 | 41 | 44.09 |
| Pathological diagnosis | | |
| Anaplastic astrocytoma | 38 | 40.86 |
| Glioblastoma multiforme | 55 | 59.14 |

## Patients and clinical specimens

The 93 paraffin-embedded high-grade glioma(grade III-IV) tissues, including 38 anaplastic astrocytoma and 55 glioblastoma multiforme samples, were obtained from the Second Affiliated Hospital of Chongqing Medical University between 2017 and 2023. All the patients' clinical information is listed in Table 1.

## Immunohistochemistry(IHC)

Paraffin sections were deparaffinized in xylene and rehydrated in ethanol at a descending concentration. Next, the sections were treated with 3% hydrogen peroxide, the antigens were retrieved in citrate buffer, the nonspecific binding was blocked with 5% goat serum for 35 min. Then, the tissues were incubated with NPRL2(1:100), TRIM16(1:100), Gal-3(1:200) and CD8(1:100) antibodies overnight at 4℃. After incubation with secondary antibodies at 37℃ for 40 min, the tissues were stained with diaminobenzidine and counterstained with hematoxylin. The isotype controls, IgG from the same species of primary antibodies, were processed along with the samples. No apparent immunoreactivity was observed in isotype controls. Finally, the slides were examined under a microscope(DM6000 B; Leica, Wetzlar, Germany). The NPRL2, TRIM16, Gal-3 and CD8 positive cellular percentages in each sample were estimated as follows: Five nonoverlapping fields of vision were selected randomly in one slice, and the numbers of positively expressed cells(brown stain) and total cells(blue stain) were calculated to obtain the ratio of positive cells to total cells in each field of vision. The average of five ratios was considered as percentage of positive cells in one patient.

## Statistical analysis

Significant differences were identified using *t*-Test, ANOVA, Kruskal-Wallis multiplex analysis, and Pearson correlation coefficients. The analyses were performed by SPSS 25.0, and $P<0.05$ was considered as the statistical significance.

## Results

### NPRL2 degraded Gal-3 and reduced Gal-3 release

The NPRL2 overexpression plasmid was generated by PCR and cloned into pCMV-EGFP-MCS-Puro vector using a forward primer (5′-TGGACGAGCTGTACAAGAAGCTTGG AGGAGGGGGAA GC-3′) and a reverse primer (5′-GTG CTGGATATCTGCAGAATTCTCACTTCCAGCAGATGA TGAT-3′). The plasmid with NPRL2 gene or empty clones were transfected into 293T cells and incubated with serum-free medium plus lipofectamine 2000 for 8 h. The medium was replaced with complete medium for extra 48 h. Lentiviral particles (LV-NPRL2 and NC) were harvested and transduced into glioma cells($6 \times 10^4$ glioma cells in six-well plates and 5 μg/ml polybrene). Finally, puromycin (2 μg/ml) was used to purify these cells. WB analysis showed that NPRL2 expression was increased in LV-NPRL2 group(Fig. S1). Unexpectedly, NPRL2 overexpression suppressed Gal-3 protein(Fig. 1A), but not mRNA levels(Fig.S2). Therefore, we speculated that the effect of NPRL2 on the inhibition of Gal-3 could be attributed to post-transcriptional processes. Gal-3 release from glioma cells was also decreased in LV-NPRL2 group(Fig. 1B). CHX(50 μg/ml for 6 h) was used to block protein synthesis in order to observe Gal-3 protein stability after upregulation of NPRL2, the results found that overexpression of NPRL2 decreased the half-life of Gal-3, leading to instability of Gal-3 protein(Fig. 1C). Next, glioma cells were treated with proteasome inhibitor MG132(10μM for 6 h) to block proteasome pathway. As shown in Fig. 1D, NPRL2 significantly declined the protein levels of Gal-3 in the absence of MG132, but the downregulation of Gal-3 was attenuated in the presence of MG132, suggesting that NPRL2 induced Gal-3 protein instability via a proteasome-dependent pathway. Furthermore, ELISA also exhibited that NPRL2 overexpression inhibited Gal-3 release, which was partially reversed by MG132(Fig. 1E). These results indicated that NPRL2 repressed Gal-3 via proteasome pathway and impeded Gal-3 release.

### NPRL2 inactivated ERK1/2 and promoted TRIM16-mediated Gal-3 ubiquitination degradation

We extended our study to survey the reasons for NPRL2-induced Gal-3 degradation. HA-tagged UB plasmids were introduced into glioma cells with or without upregulation of NPRL2, followed by IP with IgG or Gal-3 antibody. NPRL2 overexpressing cells underwent heavy ubiquitination of Gal-3, whereas the NC cells displayed a light UB ladder(Fig. 2A). However, Co-IP analysis did not uncover that NPRL2 bound to Gal-3(Fig. S3). Interestingly, we verified that the E3 ligase TRIM16 was increased by NPRL2(Fig. 2B). Two glioma cell lines were transduced with TRIM16-shRNA-LV and NC1, WB analysis unveiled that TRIM16 expression was decreased by TRIM16-shRNA-LV(TRIM16-shRNA), coupled with elevated Gal-3(Fig. 2C and S4). Besides, glioma cells were divided into the NC, LV-NPRL2, LV-NPRL2 + NC1 and LV-NPRL2 + TRIM16-shRNA groups. The data confirmed that NPRL2 inhibited Gal-3 expression, which could be partially restored by TRIM16 downregulation, indicating that the ability of NPRL2 to repress Gal-3 was dependent on TRIM16(Fig. 2D). To identify whether TRIM16 facilitates Gal-3 ubiquitination degradation, Flag-empty vector and Flag-TRIM16 vector were transfected into glioma cells. After IP with Flag, we demonstrated that Flag-TRIM16 connected with Gal-3 but not with NPRL2(Fig. 2E). IF also showed colocalization between TRIM16 and cytoplasmic Gal-3(Fig. 2F). In addition, the data also explained that TRIM16 promoted Gal-3 ubiquitination(Fig. 2G). Next, the mechanism involved in the regulatory effect of NPRL2 on TRIM16 was investigated. WB analysis revealed that NPRL2 decreased p-ERK1/2 levels and increased TRIM16 levels, but the addition of an ERK1/2 activator(α-ERK1/2) diminished TRIM16 expression (Fig. 2H). These data confirmed that NPRL2 enhanced TRIM16 expression via inactivation of ERK1/2, contributing to TRIM16-mediated ubiquitination degradation of Gal-3.

### Correlation among NPRL2, TRIM16, Gal-3 and CD8+T cell accumulation in human glioma samples

We analyzed the clinical correlation of NPRL2 with TRIM16 or Gal-3 in 93 paraffin-embedded human high-grade glioma tissues via IHC. In these samples, NPRL2 expression was positively associated with TRIM16 expression, but negatively correlated with Gal-3 expression(Fig. 3A and C). As a TSG identified in our previous article, NPRL2 expression was decreased in astrocytoma and negatively correlated with histological grade, resulting in an unfavorable prognosis [5]. Accordingly, we speculated that Gal-3 was upgraded by the loss of NPRL2 and promoted glioma progression. Some studies reported that Gal-3 functioned as an immunosuppressive cytokine in the TME. As well known, $CD8^+$T cells are the ultimate immune effectors against tumors, and inactivation of $CD8^+$T cells causes failure of antitumor immunity [25]. Thus, we aimed to further detect the correlation between Gal-3 and $CD8^+$T cell accumulation. As depicted in Fig. 3A and D, Gal-3 was negatively associated with $CD8^+$T cell accumulation, indicating that Gal-3 could have an adverse effect on $CD8^+$T cells in TME.

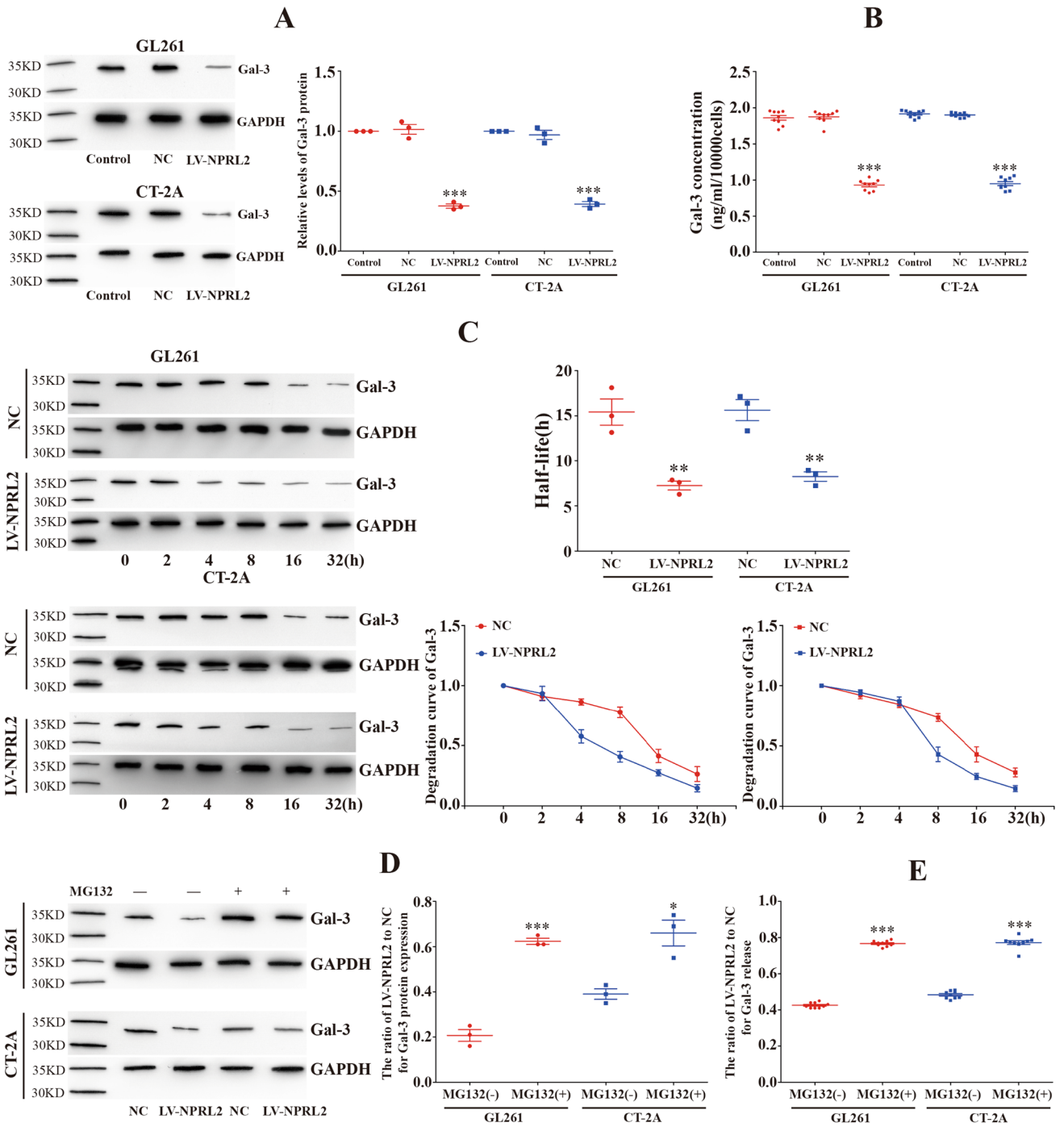


**Fig. 1** NPRL2 promoted Gal-3 degradation and reduced Gal-3 release. **A**. The expression of Gal-3 protein in control, NC and LV-NPRL2 groups($n=3$, Mean ± SD. $P<0.001^{***}$, compared with control). **B**. The release of Gal-3 protein in control, NC and LV-NPRL2 groups($n=9$, Mean ± SEM. $P<0.001^{***}$, compared with control). **C**. NPRL2 shortened Gal-3 half-life time($n=3$, Mean ± SD. $P<0.01^{**}$, compared with NC). **D**. The ratio of LV-NPRL2 to NC for Gal-3 protein expression with or without MG132($n=3$, Mean ± SD. $P<0.05^{*}$; $P<0.001^{***}$, compared with absence of MG132). **E**. The ratio of LV-NPRL2 to NC for Gal-3 protein release with or without MG132($n=9$, Mean ± SEM. $P<0.001^{***}$, compared with absence of MG132)

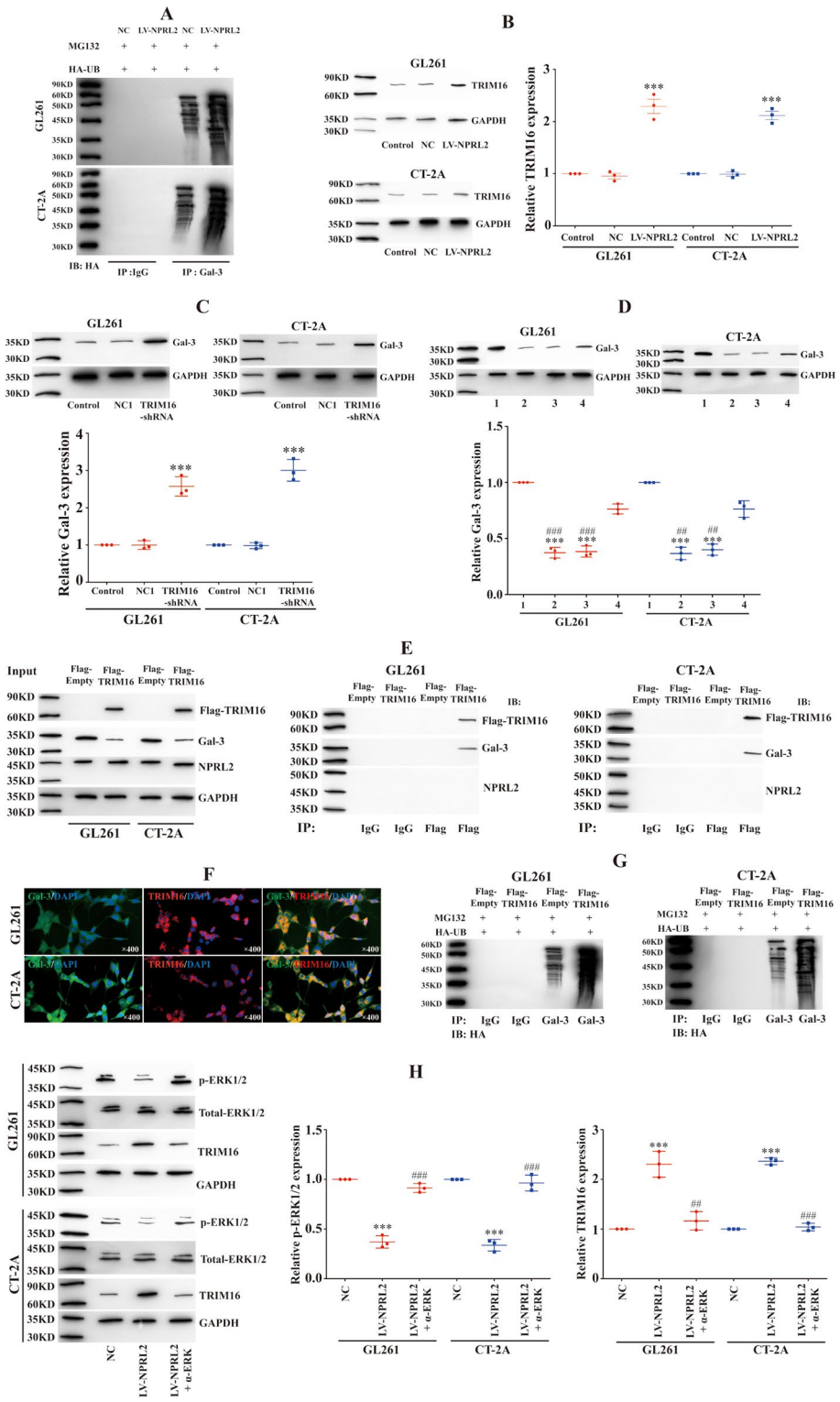


**Fig. 2** NPRL2 inhibited phospho-ERK1/2 to induce TRIM16-mediated Gal-3 ubiquitination degradation. **A**. After transfecting with HA-UB and adding MG132, Co-IP was performed with IgG or Gal-3 antibody in NC and LV-NPRL2 groups, the Gal-3 ubiquitination was observed($n=3$). **B**. The protein levels of TRIM16 were investigated in control, NC and LV-NPRL2 groups($n=3$. Mean ± SD. $P<0.001^{***}$, compared with control). **C**. The protein levels of Gal-3 were explored in control, NC1 and TRIM16-shRNA-LV(TRIM16-shRNA) groups($n=3$. Mean ± SD. $P<0.001^{***}$, compared with control). **D**. Gal-3 protein was tested in NC(1), LV-NPRL2(2), LV-NPRL2 + NC1(3) and LV-NPRL2 + TRIM16-shRNA(4) groups($n=3$. Mean ± SD. $P<0.001^{***}$, compared with group 1. $P<0.01^{\#\#}$, $P<0.001^{\#\#\#}$, compared with group 4). **E**. The glioma cells were transfected with Flag-empty vector and Flag-TRIM16 vector, then IgG or Flag antibody was used for IP with Flag-TRIM16, Gal-3 and NPRL2($n=3$). **F**. IF to detect colocalization of TRIM16 and Gal-3($n=3$). **G**. After transfecting with HA-UB and adding MG132, Co-IP was done with IgG or Gal-3 antibody in FLAG-empty vector and FLAG-TRIM16 groups, the Gal-3 ubiquitination was assessed($n=3$). **H**. The glioma cells were divided into NC, LV-NPRL2 and LV-NPRL2 plus ERK1/2 activator(α-ERK1/2) groups, the levels of phospho-ERK1/2 and TRIM16 were analyzed($n=3$. Mean ± SD. $P<0.001^{***}$, compared with NC. $P<0.01^{\#\#}$, $P<0.001^{\#\#\#}$, compared with LV-NPRL2)

## Gal-3 accelerated cuproptosis in CD8+T cells

CCK-8 assays and FCM did not reveal that Gal-3 suppressed cell viability or induced early apoptosis in CD8$^+$T cells(Fig.S5A and S5B). Interestingly, colocalization of exogenous His-tagged Gal-3 and CTR1 was observed in CD8$^+$T cells after 24 h (Fig. 4A). Co-IP also uncovered that His-tagged Gal-3 interacted directly with CTR1 (Fig. 4B). CTR1 is conducive to copper import, therefore we hypothesized that Gal-3 could participate in copper metabolism in

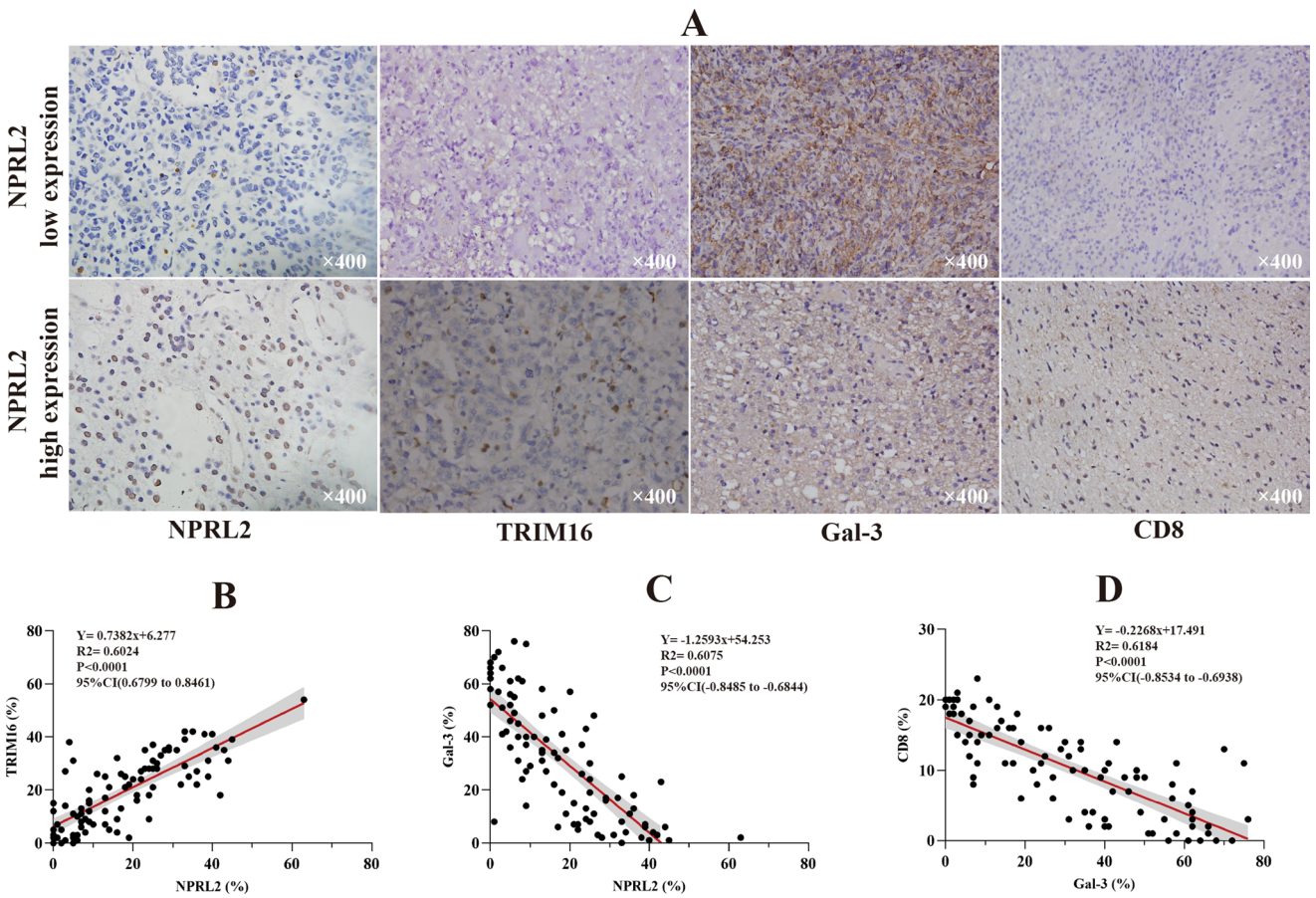


**Fig. 3** Correlation analysis of NPRL2, TRIM16, Gal-3 and $CD8^+$T cell accumulation in human glioma specimens. **A**. The expression of NPRL2, TRIM16, Gal-3 and CD8 in clinical glioma tissues. **B-D**. Pearson correlation coefficient to analyze the correlation between NPRL2 and TRIM16, NPRL2 and Gal-3, Gal-3 and CD8

$CD8^+$T cells. Elesclomol is a copper ionophore that shuttles copper into cells for copper toxicity, $CD8^+$T cell viability was not affected by 10nM, 20nM or 40nM elesclomol after 24, 48 and 72 h(Fig.S6). Next, the $CD8^+$T cells were divided into control, $CuCl_2$(10nM), $CuCl_2$(10nM) plus Gal-3(2ng/ml), 10nM elesclomol-$CuCl_2$(1:1), 10nM elesclomol-$CuCl_2$(1:1) plus Gal-3(2ng/ml). The levels of $Cu^{2+}$ in $CD8^+$T cells were increased in elesclomol-$CuCl_2$ group, and this process was further augmented by Gal-3(Fig. 4C). The elesclomol-$CuCl_2$ treatment slightly diminished $CD8^+$T cell viability at 72 h and had no impact on IL-2 or IFN-γ release. Notably, cell growth as well as IL-2 and IFN-γ secretion was significantly inhibited by elesclomol-$CuCl_2$ plus Gal-3, which ascertained that elesclomol was able to increase copper intake but not enough to cause significant cell death. However, elesclomol-$CuCl_2$ plus gal-3 markedly increased intracellular copper content and induced inactivation of $CD8^+$T cells(Fig. 4D and E). WB analysis manifested that elesclomol-$CuCl_2$ plus Gal-3 decreased DLAT and FDX1, coupled with upregulation of HSP70 (Fig. 4F). These findings suggested that Gal-3 induced cuproptosis in $CD8^+$T cells.

## NPRL2 prevented the immunosuppressive effect of Gal-3 on CD8+T lymphocytes

CM was collected to incubate with $CD8^+$T cells. Although these CMs hindered cell viability to some extent, there was no significant difference in inhibitory effect among the three groups without elesclomol-$CuCl_2$, illustrating that glioma-derived CM inhibited $CD8^+$T cell activation regardless of NPRL2 levels(**Fig.**S7). When 10nM elesclomol-$CuCl_2$(1:1) was introduced to CM, CCK-8 assays and ELISA showed that cell viability and cytokines(IFN-γ and IL-2) levels were increased in CM-LV group compared with CM-control and CM-NC groups, but the CM-LV induced-restoration was neutralized by exogenous Gal-3 protein(Fig. 5A and B). Glioma cells(control, NC and LV-NPRL2) were seeded into mouse brains, IHC unraveled that NPRL2 augmented the accumulation of $CD8^+$ T cells in the TME, but these effects could be counteracted by Gal-3 protein(Fig. 5C). These data

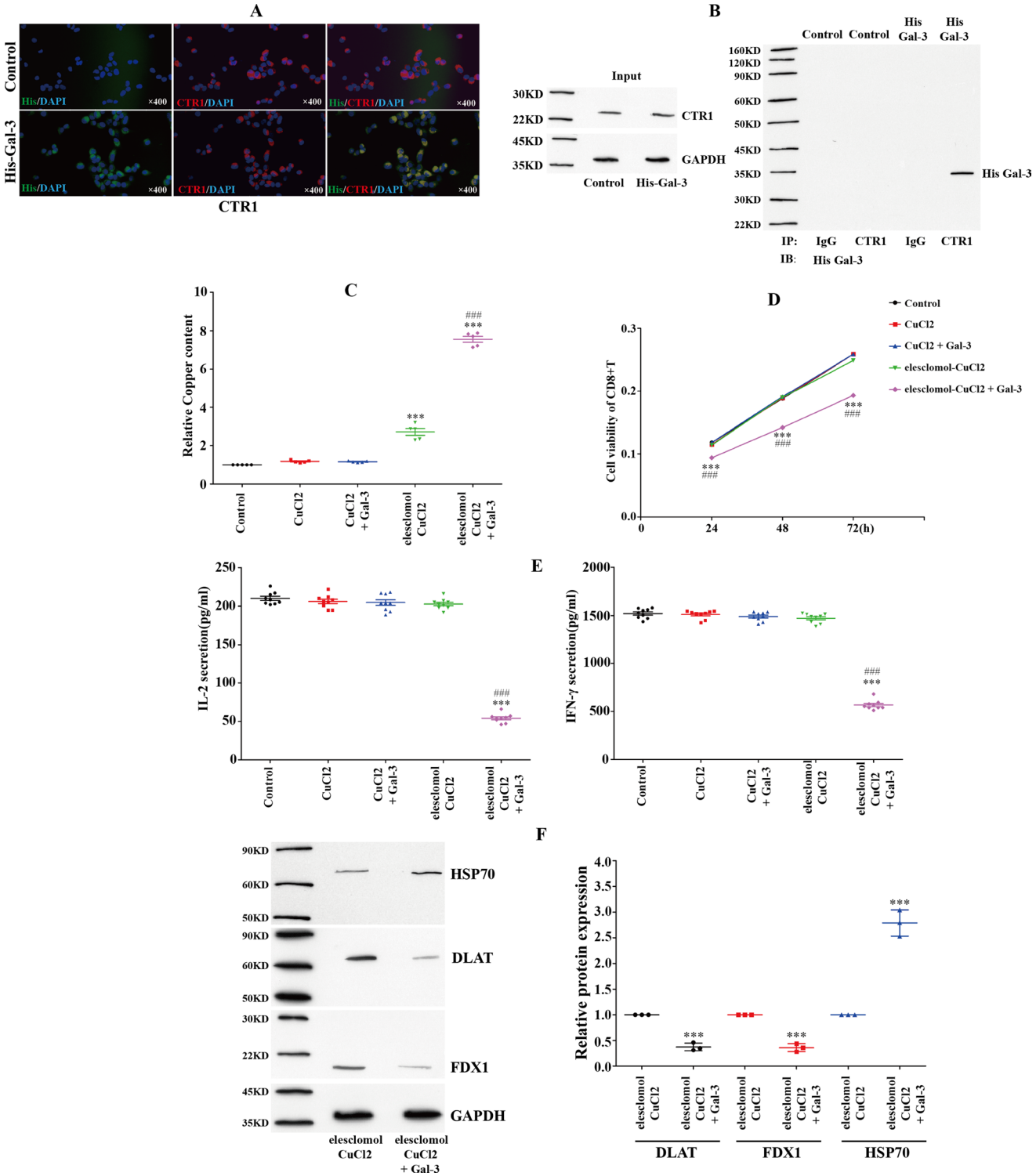


**Fig. 4** Gal-3 induced cuproptosis in CD8$^+$T lymphocytes. **A**. IF to detect the colocalization of His-tagged Gal-3 and CTR1($n=3$). **B**. Co-IP to observe the link between His-tagged Gal-3 and CTR1 in CD8$^+$T cells($n=3$). **C**. The cellular relative copper contents were tested by spectrophotometry ($n=5$. Mean ± SEM). **D**. CCK-8 to analyze cell viability($n=5$. Mean ± SEM). **E**. ELISA to calculate the IL-2 and IFN-γ secretion from CD8$^+$T cells($n=9$. Mean ± SEM). For **C**, **D**, **E**, $P^{***}<0.001$, vs. control; $P^{\#\#\#}<0.001$, vs. elesclomol-$CuCl_2$ group. **F**. WB to evaluate the different levels of HSP70, DLAT and FDX1 protein between elesclomol-$CuCl_2$ and elesclomol-$CuCl_2$ plus Gal-3 groups($n=3$. Mean ± SD. $P^{***}<0.001$, vs. elesclomol-$CuCl_2$ group)

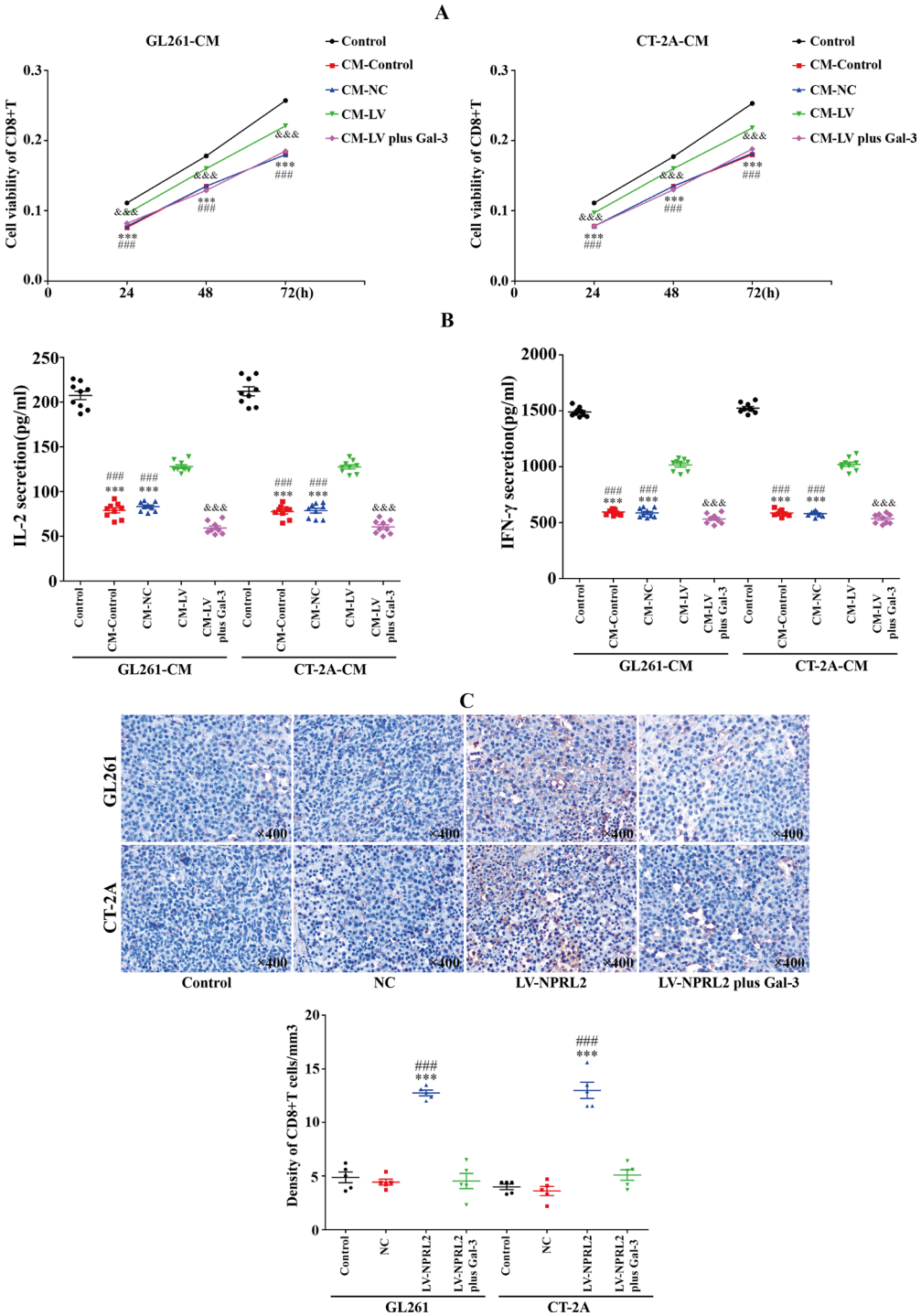


**Fig. 5** NPRL2 activated CD8$^+$T cells via suppression of Gal-3. **A**. CD8 + T cells were divided into control, CM-control, CM-NC, CM- LV, and CM-LV plus Gal-3 groups, and elesclomol-$CuCl_2$ was added into CM, the cell viability was tested at 24, 48 and 72 h($n = 5$. Mean ± SEM). **B**. The concentrations of IL-2 and IFN-γ secreted from CD8$^+$T cells were calculated after 48 h($n = 9$. Mean ± SEM). (For **A** and **B**, $P^{***} < 0.001$, vs. Control. $P < 0.001^{\#\#\#}$, vs. CM-LV. $P < 0.001^{\&\&\&}$, compared between CM-LV and CM-LV plus Gal-3). **C**. The glioma cells in control, NC, LV-NPRL2, LV-NPRL2 plus Gal-3 protein groups were injected into mouse brain to establish intracranial tumor, and CD8$^+$T cell accumulation was assessed at 21d($n = 5$. Mean ± SEM. $P^{***} < 0.001$, vs. Control. $P < 0.001^{\#\#\#}$, vs. between LV-NPRL2 and LV-NPRL2 plus Gal-3)

confirmed that NPRL2 prevented Gal-3 induced-cuproptosis and promoted the immunological activity of $CD8^+$T lymphocytes.

## Discussion

The NPRL2 gene is harbored in chromosome 3p21.3 where allelic loss, homozygous deletion or loss of heterozygosity often appears in a variety of tumors [5]. As a result, NPRL2 expression is decreased and the TSG functions are attenuated, giving rise to tumorigenesis, invasion, drug tolerance, relapse and poor outcomes [26–28]. We verified that NPRL2 impaired the cell cycle of glioma via inactivation of the PDK1-AKT1 signaling pathway [5]. However, a recent study proposed that NPRL2 was negatively associated with the infiltration score of immune cells in the TME, and high levels of NPRL2 were more responsive to immunotherapy [28].

To further elucidate the role of NPRL2 in TME, we first identified that NPRL2 repressed Gal-3 expression and release from glioma cells through ubiquitination, which was responsible for modulating the "quality" and "quantity" of substrate proteins related to malignant tumors [29]. Other literature described that NPRL2 physically interacted with E3 ligases to regulate protein stability [6]. In addition, previous reports showed that the E3 ligase TRIM16 directly connected with Gal-3 for ubiquitination degradation [18]. Thus, we attempted to survey the interactions among the three proteins and the results corroborated that TRIM16 was able to degrade Gal-3 via ubiquitination. However, NPRL2-induced E3 ligase activity of TRIM16 did not rely on combination between each other. Alternatively, we witnessed that NPRL2 promoted TRIM16 via the inhibition of phospho-ERK1/2, which in turn decreased Gal-3 expression and release through TRIM16-dependent ubiquitination degradation. Combined with our previous research, NPRL2 is a critical component that regulates different downstream signal transduction pathway in glioma.

The levels of Gal-3 were elevated in astrocytoma [30]. Subsequently, clinical glioma specimens were collected to analyze the correlation between these proteins. Given the reduced NPRL2 in glioma documented in our previous study, the IHC figured out that NPRL2 levels were positively associated with TRIM16 and negatively correlated with Gal-3 [5]. Hence, we deemed that downregulation of NPRL2 increased Gal-3 levels. In fact, Gal-3 is considered as a pleiotropic tumor relevant protein and deserves particular attention in immuno-oncology [15]. Some papers have confirmed that Gal-3 negatively influenced antitumor immunity, patients with Gal-3-negative tumors showed better therapeutic responses, and Gal-3 blockade augmented the antitumor efficacy of immune checkpoint inhibitors [31–33]. Importantly, our data also unveiled that Gal-3 was negatively associated with $CD8^+$T cell accumulation, indicating that the absence of NPRL2 enhanced Gal-3 and resulted in immune evasion.

Some articles have shown that Gal-3 induced $CD8^+$T cell apoptosis and hindered $CD8^+$T cell viability as well as recruitment to the TME [34–36]. However, cytotoxicity was not detected after exposure to extra Gal-3 protein. The reason for inconsistency may be attributed to the different concentrations which required for much higher to provoke $CD8^+$T cell apoptosis [34]. IF and Co-IP displayed that Gal-3 was directly linked to CTR1 which is the most important influx transporter of copper ions. The copper was an endogenous metal necessary for numerous biological functions, and intracellular copper was typically restricted to extraordinarily low levels depending on import and export balance [37]. Recently, a breakthrough was made that excess intracellular copper triggered a unique type of death with mitochondrial dysregulation, namely cuproptosis [21]. Next, we explored the effects of Gal-3 on copper metabolism in $CD8^+$T cells and found that Gal-3 significantly increased the levels of intracellular copper when copper ionophore elesclomol were added. Furthermore, increased copper restrained cell viability and immune related cytokines, coupled with the characteristics of cuproptosis, including decreased FDX1 and DLAT as well as increased HSP70.

Ultimately, the anticancer efficacy of NPRL2 was evaluated in terms of tumor immunity. Upregulation of NPRL2 in glioma promoted $CD8^+$T cell infiltration into the TME and restored immunocompetence in vitro and in vivo, which could be counteracted by extra Gal-3. We concluded that NPRL2 improved immunosurveillance in glioma by inhibiting Gal-3 mediated $CD8^+$T cell cuproptosis. However, Gal-3 also played indispensable role in immunosuppression via multiple mechanisms, such as memory T-cell inactivation, M2 macrophage polarization, dysregulation of dendritic cell, enrichment of myeloid-derived suppressor cells [16, 38, 39]. Consequently, further research must be performed to highlight the role of NPRL2/TRIM16/ Gal-3 axis in regulation of the tumor immune microenvironment.

## Conclusion

In summary, we substantiated that overexpression of NPRL2 in glioma cells impeded $CD8^+$T cell cuproptosis in favor of immunological activity by promoting the TRIM16-mediated ubiquitination degradation of Gal-3. Our identification indicated that targeting the NPRL2/TRIM16/Gal-3 axis will be a prominent achievement for advances in glioma immunotherapy.

**Supplementary Information** The online version contains supplementary material available at https://doi.org/10.1007/s00018-024-05454-2.

**Acknowledgements** Not applicable.

**Author contributions** NH and JC designed this study. FW, JHY, MXZ and YYW performed experiments. MYS, XL and HZ analyzed the data. FW wrote the manuscript. YC revised the manuscript.

**Funding** Postdoctoral program of the Chongqing Natural Science Foundation Project(CSTB2023NSCQ-BHX0042, CSTB2023NSCQ-BHX0068). Project of the Second Affiliated Hospital of Chongqing Medical University(kryc-yq-2216, kryq-yq-2107, kryc-gg-2110). The Chunhui Plan of National Educational Ministry(HZKY20220218).

**Data availability** All data generated or analyzed during this study are included in this published article[and its supplementary information files].

## Declarations

**Ethics approval** All animal studies and use of paraffin-embedded glioma samples were approved by the Ethics Committee of Chongqing Medical University(IACUC-CQMU-2023-0447).

**Consent for publication** Not applicable.

**Conflict of interest** The authors declare that they have no competing interests.



## References

1. Ran X, Zheng J, Chen L, Xia Z, Wang Y, Sun C et al (2024) Single-cell Transcriptomics reveals the heterogeneity of the Immune Landscape of IDH-Wild-Type High-Grade Gliomas. Cancer Immunol Res 12:232–246
2. Bausart M, Préat V, Malfanti A (2022) Immunotherapy for glioblastoma: the promise of combination strategies. J Exp Clin Cancer Res 41:35
3. Yang F, Akhtar MN, Zhang D, El-Mayta R, Shin J, Dorsey JF et al (2024) An immunosuppressive vascular niche drives macrophage polarization and immunotherapy resistance in glioblastoma. Sci Adv 10:eadj4678
4. Jackson CM, Choi J, Lim M (2019) Mechanisms of immunotherapy resistance: lessons from glioblastoma. Nat Immunol 20:1100–1109
5. Huang N, Cheng S, Mi X, Tian Q, Huang Q, Wang F et al (2016) Downregulation of nitrogen permease regulator like-2 activates PDK1-AKT1 and contributes to the malignant growth of glioma cells. Mol Carcinog 55:1613–1626
6. Peng Y, Dai H, Wang E, Lin CC, Mo W, Peng G et al (2015) TUSC4 functions as a tumor suppressor by regulating BRCA1 stability. Cancer Res 75:378–386
7. Gao H, Yin J, Ji C, Yu X, Xue J, Guan X et al (2023) Targeting ubiquitin specific proteases (USPs) in cancer immunotherapy: from basic research to preclinical application. J Exp Clin Cancer Res 42:225
8. Sampson C, Wang Q, Otkur W, Zhao H, Lu Y, Liu X et al (2023) The roles of E3 ubiquitin ligases in cancer progression and targeted therapy. Clin Transl Med 13:e1204
9. Senft D, Qi J, Ronai ZA (2018) Ubiquitin ligases in oncogenic transformation and cancer therapy. Nat Rev Cancer 18:69–88
10. Fujita Y, Tinoco R, Li Y, Senft D, Ronai ZA et al (2019) Ubiquitin ligases in Cancer Immunotherapy - Balancing Antitumor and Autoimmunity. Trends Mol Med 25:428–443
11. Wang L, Zhang X, Lin ZB, Yang PJ, Xu H, Duan JL et al (2021) Tripartite motif 16 ameliorates nonalcoholic steatohepatitis by promoting the degradation of phospho-TAK1. Cell Metab 33:1372–1388e7
12. Tian H, Lian R, Li Y, Liu C, Liang S, Li W et al (2020) AKT-induced lncRNA VAL promotes EMT-independent metastasis through diminishing Trim16-dependent vimentin degradation. Nat Commun 11(1):5127
13. Ruan L, Liu W, Yang Y, Chu Z, Yang C, Yang T et al (2021) TRIM16 overexpression inhibits the metastasis of colorectal cancer through mediating snail degradation. Exp Cell Res 406:112735
14. Sturgill ER, Rolig AS, Linch SN, Mick C, Kasiewicz MJ, Sun Z et al (2021) Galectin-3 inhibition with belapectin combined with anti-OX40 therapy reprograms the tumor microenvironment to favor anti-tumor immunity. Oncoimmunology 10:1892265
15. Scafetta G, D'Alessandria C, Bartolazzi A (2024) Galectin-3 and cancer immunotherapy: a glycobiological rationale to overcome tumor immune escape. J Exp Clin Cancer Res 43:41
16. Kouo T, Huang L, Pucsek AB, Cao M, Solt S, Armstrong T et al (2015) Galectin-3 shapes Antitumor Immune responses by suppressing CD8 + T cells via LAG-3 and inhibiting expansion of Plasmacytoid dendritic cells. Cancer Immunol Res 3:412–423
17. Zhang IY, Liu S, Zhang L, Liang R, Fang Q, Zhao J et al (2023) RAGE ablation attenuates glioma progression and enhances tumor immune responses by suppressing galectin-3 expression. Neuro Oncol 25:886–898
18. Chauhan S, Kumar S, Jain A, Ponpuak M, Mudd MH, Kimura T et al (2016) TRIMs and Galectins Globally Cooperate and TRIM16 and Galectin-3 co-direct autophagy in Endomembrane Damage Homeostasis. Dev Cell 39:13–27
19. Guo Y, Shen R, Yang K, Wang Y, Song H, Liu X et al (2023) RNF8 enhances the sensitivity of PD-L1 inhibitor against melanoma through ubiquitination of galectin-3 in stroma. Cell Death Discov 9:205
20. Xie J, Yang Y, Gao Y, He J (2023) Cuproptosis: mechanisms and links with cancers. Mol Cancer 22:46
21. Tsvetkov P, Coy S, Petrova B, Dreishpoon M, Verma A, Abdusamad M et al (2022) Copper induces cell death by targeting lipoylated TCA cycle proteins. Science 375:1254–1261
22. Qin Y, Liu Y, Xiang X, Long X, Chen Z, Huang X et al (2023) Cuproptosis correlates with immunosuppressive tumor microenvironment based on pan-cancer multiomics and single-cell sequencing analysis. Mol Cancer 22:59

23. Huang N, Tang J, Yi X, Zhang M, Li B, Cheng Y et al (2024) Glioma-derived S100A9 polarizes M2 microglia to inhibit CD8 + T lymphocytes for immunosuppression via αvβ3 integrin/AKT1/TGFβ1. Biochim Biophys Acta Mol Cell Res 1871:119619
24. Huang N, Zhao G, Yang Q, Tan J, Tan Y, Zhang J et al (2020) Intracellular and extracellular S100A9 trigger epithelial-mesenchymal transition and promote the invasive phenotype of pituitary adenoma through activation of AKT1. Aging 12:23114–23128
25. Giles JR, Globig AM, Kaech SM, Wherry EJ (2023) CD8 + T cells in the cancer-immunity cycle. Immunity 56:2231–2253
26. Pastuszak-Lewandoska D, Kordiak J, Migdalska-Sęk M, Czarnecka KH, Antczak A, Górski P et al (2015) Quantitative analysis of mRNA expression levels and DNA methylation profiles of three neighboring genes: FUS1, NPRL2/G21 and RASSF1A in non-small cell lung cancer patients. Respir Res 16:76
27. Wang YC, Tsai MC, Chen YS, Hsieh PM, Hung CM, Lin HY et al (2022) NPRL2 down-regulation facilitates the growth of hepatocellular carcinoma via the mTOR pathway and autophagy suppression. Hepatol Commun 6:3563–3577
28. Pi Y, Zhan Y, Song J, Jin X, Chen J (2022) Bioinformatics analysis of the prognostic and immunotherapeutic significance of NPRL2 in stomach adenocarcinoma. J Gastrointest Oncol 13:1589–1604
29. Pi Y, Feng Q, Sun F, Wang Z, Zhao Y, Chen D et al (2023) Loss of SMURF2 expression enhances RACK1 stability and promotes ovarian cancer progression. Cell Death Differ 30:2382–2392
30. Wang H, Song X, Huang Q, Xu T, Yun D, Wang Y et al (2019) LGALS3 promotes Treatment Resistance in Glioblastoma and is Associated with Tumor Risk and Prognosis. Cancer Epidemiol Biomarkers Prev 28:760–769
31. Wu X, Giobbie-Hurder A, Connolly EM, Li J, Liao X, Severgnini M et al (2018) Anti-CTLA-4 based therapy elicits humoral immunity to galectin-3 in patients with metastatic melanoma. Oncoimmunology 7:e1440930
32. Capalbo C, Scafetta G, Filetti M, Marchetti P, Bartolazzi A (2019) Predictive biomarkers for checkpoint inhibitor-based immunotherapy: the Galectin-3 signature in NSCLCs. Int J Mol Sci 20:1607
33. Zhang H, Liu P, Zhang Y, Han L, Hu Z, Cai Z et al (2021) Inhibition of galectin-3 augments the antitumor efficacy of PD-L1 blockade in non-small-cell lung cancer. FEBS Open Bio 11:911–920
34. Stillman BN, Hsu DK, Pang M, Brewer CF, Johnson P, Liu FT et al (2006) Galectin-3 and galectin-1 bind distinct cell surface glycoprotein receptors to induce T cell death. J Immunol 176:778–789
35. Gordon-Alonso M, Hirsch T, Wildmann C, van der Bruggen P (2017) Galectin-3 captures interferon-gamma in the tumor matrix reducing chemokine gradient production and T-cell tumor infiltration. Nat Commun 8:793
36. Ruvolo PP (2016) Galectin 3 as a guardian of the tumor microenvironment. Biochim Biophys Acta 1863:427–437
37. Wang X, Chen D, Shi Y, Luo J, Zhang Y, Yuan X et al (2023) Copper and cuproptosis-related genes in hepatocellular carcinoma: therapeutic biomarkers targeting tumor immune microenvironment and immune checkpoints. Front Immunol 14:1123231
38. Curti BD, Koguchi Y, Leidner RS, Rolig AS, Sturgill ER, Sun Z et al (2021) Enhancing clinical and immunological effects of anti-PD-1 with belapectin, a galectin-3 inhibitor. J Immunother Cancer 9:e002371
39. MacKinnon AC, Farnworth SL, Hodkinson PS, Henderson NC, Atkinson KM, Leffler H et al (2008) Regulation of alternative macrophage activation by galectin-3. J Immunol 180:2650–2658